applied sciences

MDPI

Article

Potentiality of Rod-Type Chitosan Adsorbent Derived from Sewage Sludge

Ji Hae Seo †, Namgyu Kim †, Munsik Park and Donghee Park *

Department of Environmental and Energy Engineering, Yonsei University, 1 Yonseidae-gil, Wonju 26493, Republic of Korea
* Correspondence: dpark@yonsei.ac.kr; Tel.: +82-33-760-2435; Fax: +82-33-760-2571
† These authors contributed equally to this work.

Abstract: The potential use of wastewater sludge as a biosorbent for the removal of various metals and metalloids from aqueous solutions was investigated. The sludge was immobilized in a rod shape with chitosan to improve sorption capacity and solid–liquid separation ability. An optimal condition for the production of rod-shaped chitosan-immobilized sludge (RCS) was determined by considering the biosorbent production potential and As(V) removal efficiency. The optimal sludge and chitosan contents and RCS thickness were 6.0%, 4.0%, and 0.2–0.3 mm, respectively. The anion removal performance of RCS was investigated for As(V), Cr(VI), and Mn(VII), and the cation removal performance was investigated for Cd(II). Pseudo-first-order and pseudo-second-order models adequately explained the kinetic data for the RCS, while the Langmuir and Freundlich models explained the equilibrium data for the RCS. These results showed that RCS has a higher adsorption capacity for anions than for cations. The results also indicated that electrostatic attraction or ion exchange is the main mechanism for metal/metalloid removal by RCS, except for the case of Mn(VII) where an adsorption-coupled reduction mechanism may be suggested.

Keywords: sewage sludge; biosorption; chitosan; arsenic; mechanism

check for updates

Citation: Seo, J.H.; Kim, N.; Park, M.; Park, D. Potentiality of Rod-Type Chitosan Adsorbent Derived from Sewage Sludge. *Appl. Sci.* **2023**, *13*, 2055. https://doi.org/10.3390/app13042055

Academic Editors: Marco Carnevale Miino and Maria Cristina Collivignarelli

Received: 26 December 2022
Revised: 29 January 2023
Accepted: 31 January 2023
Published: 4 February 2023

Copyright: © 2023 by the authors. Licensee MDPI, Basel, Switzerland. This article is an open access article distributed under the terms and conditions of the Creative Commons Attribution (CC BY) license (https://creativecommons.org/licenses/by/4.0/).

1. Introduction

The use of heavy metals has increased with industrial development, and the possibility of these heavy metals being released into the environment has also increased. Due to their detrimental effects on human health, finding methods to remove heavy metals is very important. Chemical precipitation, ion exchange, evaporation, electroplating, and membrane processes are common commercial methods for removing heavy metals from aqueous solutions [1,2]. However, these methods are expensive, inefficient, and can produce chemical sludge. New green technologies for removing heavy metals from wastewater are urgently needed.

Recently, biosorption has been suggested as a possible alternative to conventional methods for heavy metal removal [3]. The main advantages of biosorption are reusability, low operating cost, and no generation of toxic secondary compounds. Biosorbents can be prepared from a variety of biomass such as algae, aquatic plants, moss, and bacteria. Many studies have been carried out to produce a biosorbent using wastewater sludge, which places no limitation on the production amount [4–7]. Unlike the case of using microorganisms, wastewater sludge does not require cultivation and is advantageous for commercial production because it is generated in large quantities. Despite the advantages, the use of wastewater sludge itself has several drawbacks. The main limitations include solid–liquid separation problems, possible biomass swelling, and the inability to regenerate/reuse it [3,8]. Therefore, in order to overcome these drawbacks, wastewater sludge must be immobilized. Chitosan, sodium alginate, polysulfone, polyacrylamide, and polyurethane have been used as matrix materials for the immobilization of biosorbents [9,10]. Special

attention has been given to polysaccharides and natural polymers such as chitosan, which is an emerging matrix material for immobilizing biomass [11].

In this study, sewage sludge waste was used as a raw material for the manufacture of biosorbents for the removal of heavy metals from aqueous solutions by batch biosorption experiments. To facilitate solid–liquid separation, sludge was immobilized by chitosan, which is known as a common, inexpensive, and environmentally friendly matrix material. Fourier transform infrared spectroscopy (FTIR) analysis was performed and total organic carbon (TOC) measurements were taken to confirm immobilization strength and characteristics. Kinetic and isotherm experiments were conducted to evaluate the removal rate and capacity of the biosorbent.

2. Materials and Methods

2.1. Preparation of the Rod-Type Biosorbent

The raw material used in the experiments was sludge waste from a biological wastewater treatment plant at Yonsei University, Korea. The sludge consisted of an average of $15 \pm 5\%$ total solids and $70 \pm 5\%$ volatile solids/total solids. The immobilization process was initiated with 2–6% (w/v) activated sludge (ignoring moisture) stirred in distilled water. After mixing, a 3–6% (w/v) solution of chitosan and 5% acetic acid (v/v) was added by continuous stirring with a mechanical stirrer at 160 rpm for 24 h. The mixture was extruded through syringes (0.2–0.3 mm, 0.5–0.6 mm, 0.8–0.9 mm, and 1.0–1.2 mm in diameter) into 2 M sodium hydroxide. The resultant rod-type biosorbent was kept in a polymerizing medium for 4 h. In order to compare the types of biosorbents, bead-type biosorbent was also prepared using the same process. The biosorbents were washed with distilled water to leach out excess solvents and then freeze-dried. The dried biosorbents were stored in a desiccator until used in experiments.

2.2. Reagents

Chitosan (75–85% acetylation degree, molecular weight: 200–800 kDa) was supplied by Sigma-Aldrich (USA). Acetic acid (purity > 99%) was purchased from Duksan (Ansan, Korea). Pure analytical grade As(V), Cd(II), Cr(VI), and Mn(VII) solutions were prepared by dissolving solid $Na_2HAsO_4 \cdot 7H_2O$ (Sigma-Aldrich, St. Louis, MO, USA), $Cd(NO_3)_2 \cdot 4H_2O$ (Sigma-Aldrich, USA), $K_2Cr_2O_7$ (Junsei, Tokyo, Japan), and $KMnO_4$ (Samchun, Gyeonggi-do, Korea) in distilled water. That is, As(V), Cr(VI), and Mn(VII) were present in anionic form (($HAsO_4^{-2}$, $Cr_2O_7^{-2}$, MnO_4^{-1}), and Cd(II) in cationic form (Cd^{2+}). All chemicals used in this study were of analytical grade. The pH of the solutions was adjusted by adding sodium hydroxide (Samchun, Korea) or hydrogen chloride (Samchun, Korea) solution.

2.3. Batch Adsorption Studies

Kinetic and isothermal removal of As(V), Cd(II), Cr(VI), and Mn(VII) from aqueous solutions by biosorbent rods were observed in 230 mL plastic bottles. The equilibration (shaking) time was 6 h in contact with 200 mL of the wastewater. The bottles were agitated in a shaker at 200 rpm at room temperature. In the kinetics experiment, 2.0 g/L of each biosorbent was put into contact with 50 mg/L of each metal or metalloid solution. All solutions were adjusted to pH 5.5. As shown in Figure S1, the biosorbent showed poor acid resistance below pH 5, so all batch experiments were conducted at pH 5.5. Through the precipitation experiment of each metal according to pH, it was confirmed that none of the metals used in this study precipitated at pH 5.5. In all batch experiments, the solution pH was maintained at the desired value (pH 5.5) using 1 M HCl and 1 M NaOH solutions. Isotherm experiments were carried out at various metal concentrations, ranging from 50 mg/L to 1500 mg/L. Since many studies have suggested heavy metal wastewater concentrations in the range of tens to hundreds of mg/L, experiments were conducted at those concentrations. The amount of metal or metalloid adsorbed on the biosorbent, q (mg/g), was calculated using the mass balance equation

$$q\ (mg/g) = \frac{(C_0 - C_e)V}{m} \quad (1)$$

where C_0 and C_e are the initial and equilibrium concentrations (mg/L), respectively, V is the working volume (L), and m is the weight of the biomass (g). All biosorption experiments were performed in triplicate, with an error rate of less than 5%. Mean values were used for kinetic and isotherm experimental data.

2.4. Analytical Methods

The TOC of the solution was measured using a TOC analyzer (TOC-VCPH/CPN, Shimadzu, Kyoto, Japan). Total nitrogen (TN) and total phosphorous (TP) were determined using a test kit (C-MAC. Co., Daejeon, Korea). An infrared spectrum of the biosorbent was obtained with an FTIR spectrometer (Vertex 70, Bruker, Billerica, MA, USA). An inductively coupled plasma optical emission spectrometer (ICP/IRIS, Thermo Jarrell Ash Co., Waltham, MA, USA) was used to analyze As, Cd, Cr, and Mn after being filtered through a 0.20 µm membrane [12]. The Cr(VI) concentration was determined by spectrophotometric analysis at 540 nm according to a standard method using 1,5-diphenylcarbazide [13]. The pink color of Mn(VII) was analyzed at 525 nm to measure its concentration [14].

3. Results and Discussion

3.1. Characteristics of Chitosan-Immobilized Biosorbent

Since activated sludge is composed of bacteria and protozoa, biosorbents made directly from the sludge may unintentionally contaminate water systems [15]. Immobilization technology can solve this problem. In this study, biosorbents were prepared by an immobilization technique using chitosan. In recent years, many studies have focused on immobilization with chitosan, but few studies have attempted to evaluate the immobilization performance. Immobilization performance was tested by analyzing the TOC released from the biosorbent during pretreatment with deionized water. As a result, the TOC released from the immobilized biosorbent was much lower than that of raw sludge. In addition, TN and TP, which are indicators of water pollution, were also found to be less eluted (Table 1), suggesting that immobilization can alter the properties of a biosorbent, including surface functional groups. In particular, functional groups on the surface often change after immobilization. To characterize the changes in functional groups, FTIR analysis was used to investigate raw sludge and chitosan-immobilized biosorbent (Figure S2). The spectra of raw sludge and chitosan-immobilized biosorbent showed many absorption peaks. A broad and strong band in the 3600–3200 cm^{-1} region was associated with NH and OH stretching vibrations in the amine and hydroxyl groups [16]. Both spectra also showed absorption peaks at 1650 cm^{-1} and 1750 cm^{-1} relevant to the stretching band of the carboxyl double bond in the carboxyl functional group [17]. The phosphate group was also observed (1150 cm^{-1} (=O stretching) and 1050 cm^{-1} (POH stretching and/or POC stretching)) [18]. After the fixation of the sludge with chitosan, a slight change occurred in the FTIR spectrum. The band at 3378 cm^{-1} was broadened due to the abundance of amine groups in chitosan. Amine groups play the most important role in anion removal by biosorption [19]. The FTIR results show that chitosan-immobilized biomass was expected to remove anions more effectively than raw biomass [20].

Table 1. Values of TN, TP, TOC, and TC released from raw sludge and sludge–chitosan (experimental condition: sample dosage 2 g/L, solution volume 200 mL, and elution time 12 h).

	Biosorbent Type	
	Raw Sludge	**Sludge–Chitosan**
TN (mg-N/L)	30.46	3.60
TP (mg-P/L)	11.63	1.28
TOC (mg-C/L)	26.66	5.02
TC (mg-C/L)	43.77	6.72

3.2. Optimization of Rod-Type Biosorbent Modification Conditions

The biosorbent manufacturing conditions were optimized by manipulating the biosorbent shape, sludge content, chitosan content, and diameter of the biosorbent.

3.2.1. Effect of Biosorbent Shape

A kinetic study was performed to determine the effect of immobilization and biosorbent shape on adsorption. Experiments using raw sludge (RS), bead-type chitosan-immobilized sludge (BCS), and rod-type chitosan-immobilized sludge (RCS) were performed to evaluate the contact time required to reach equilibrium. Chitosan is a biopolymer with a high nitrogen content that confers an adsorption ability on anionic metal ions. As(V) was used to evaluate the anionic metal removal performance of each biosorbent. Figure 1a shows the removal of As(V) by RS, BCS, and RCS as a function of contact time at pH 5.5. BCS and RCS showed 2–3 times higher As(V) removal efficiency than RS. This result is due to the presence of amine groups on the biosorbent [13].

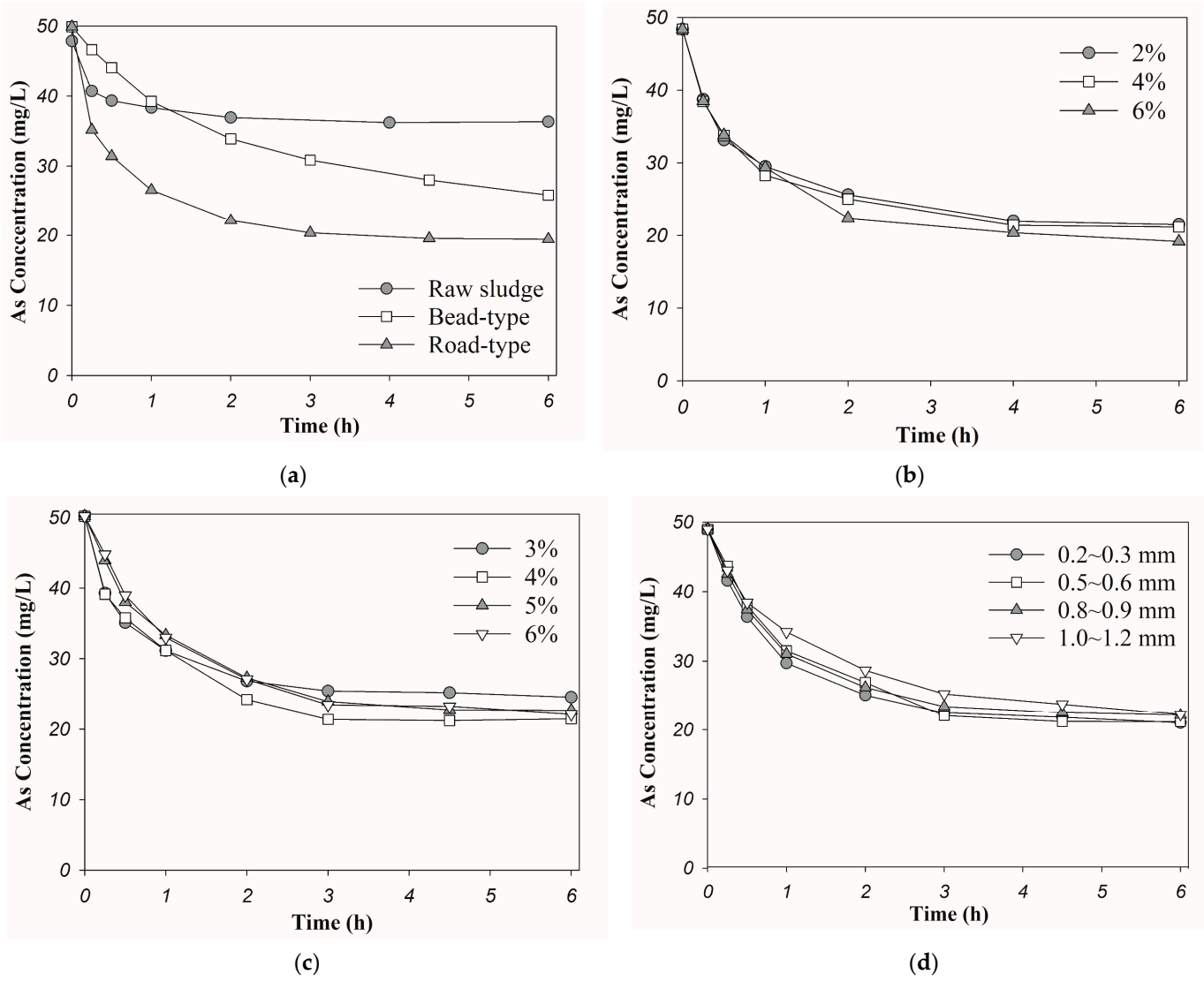

Figure 1. Effect of (**a**) biosorbent shape, (**b**) chitosan content, (**c**) sludge content, and (**d**) biosorbent size on the adsorption of As(V) on the sludge–chitosan (biosorbent dosage = 2 g/L, agitation rate = 200 rpm, contact time = 6 h, temperature = 25 °C, Vw = 200 mL, and pH non shift (pH 5.5)).

3.2.2. Effect of Material Content in Biosorbent

The amounts of sludge and chitosan were important variables affecting sorption performance. Figure 1b shows the effects of sludge content on As(V) removal onto RCS. The sludge content affected the biosorbent surface and thus the As(V) removal capacity of the biosorbent. For further details, adsorption results were compared with pseudo-first-order and pseudo-second-order kinetics modeling. These models have been employed to investigate the adsorption dynamics of pollutants onto the biosorbents in relation to time and to estimate the rate of the process. They also help explain biosorption mechanisms and potential rate-controlling steps that may include mass transport and chemical reaction processes [21]. The pseudo-first-order equation is:

$$q_t = q_e\left(1 - e^{-k_1 t}\right) \tag{2}$$

where q_e is the amount of adsorbate adsorbed (mg/g) at equilibrium, q_t is the amount of adsorbate adsorbed (mg/g) at time t (min), and k_1 (min^{-1}) is the rate constant.

The pseudo-second-order equation is usually associated with a situation in which the rate of direct adsorption or desorption controls the overall sorption kinetics, and typically describes the removal behavior of metals [22,23]. An integrated form of the pseudo-second-order equation can be expressed as:

$$\frac{t}{q_t} = \frac{1}{k_2 \cdot {q_e}^2} + \frac{t}{q_e} \tag{3}$$

or

$$\frac{q_t}{t} = \frac{h}{1 + k_2 q_e t} \tag{4}$$

where h (g/mg·h) is the initial sorption rate and k_2 (g/mg·h) is the rate constant. The rate constant, initial sorption rate, and modulus values were calculated from different equilibrium metal sorption equations and are shown in Table 2. Equilibrium uptake (q_e) increased with increasing sludge fraction in RCS. Comparing the rate constant and initial adsorption rate, RCS containing 4.0% sludge showed the fastest adsorption rate. From these results, it can be seen that 4.0% was satisfactory in terms of speed, but 6.0% was the optimal adsorption amount. In order to increase adsorption capacity, it was decided to produce an adsorbent containing more than 6.0% sludge. In this study, the optimal sludge content was determined to be 6.0% because more weight was placed on adsorption capacity.

Table 2. Comparison of pseudo-first-order model and pseudo-second-order model parameter values for different sludge contents, chitosan contents, and diameters of the biosorbent.

Sludge Content (%)	Chitosan Content (%)	Diameter (mm)	Pseudo-First-Order			Pseudo-Second-Order			
			K_1 (1/h)	q_e (mg/g)	R^2 (-)	K_2 (g/mg·h)	q_e (mg/g)	R^2 (-)	h (mg/g·h)
2.0	**4.0**	**0.2–0.3**	0.96	0.09	0.9889	0.13	14.64	0.9995	28.65
4.0	**4.0**	**0.2–0.3**	1.13	0.08	0.9855	0.14	14.84	0.9995	29.94
6.0	**4.0**	**0.2–0.3**	0.79	0.09	0.9636	0.11	16.08	0.9990	27.33
6.0	**3.0**	**0.2–0.3**	0.84	0.12	0.9395	0.19	13.69	0.9996	35.55
6.0	**4.0**	**0.2–0.3**	1.58	0.06	0.9422	0.10	16.66	0.9956	27.63
6.0	**5.0**	**0.2–0.3**	1.28	0.06	0.9628	0.07	16.16	0.9963	18.48
6.0	**6.0**	**0.2–0.3**	0.78	0.08	0.9475	0.06	16.69	0.9931	16.55
6.0	**4.0**	**0.2–0.3**	0.81	0.09	0.9759	0.09	15.78	0.9984	22.42
6.0	**4.0**	**0.5–0.6**	1.63	0.04	0.9192	0.06	16.82	0.9916	16.13
6.0	**4.0**	**0.8–0.9**	0.95	0.08	0.9969	0.08	15.47	0.9971	19.47
6.0	**4.0**	**1.0–1.2**	0.64	0.08	0.9911	0.06	15.70	0.9992	14.84

The effect of chitosan content in RCS on the biosorption of As(V) is shown in Figure 1c. The values of the variables used in Equations (2)–(4) are shown in Table 2. Chitosan content of 6.0% in RCS resulted in higher As(V) removal compared to other RCS. The higher removal may be due to the effect of As(V) on the amine group of chitosan in RCS. When comparing correlation coefficients (R^2), the pseudo-second-order kinetic model was better suited to describing the biosorption kinetics of the RCS. The As(V) adsorption process was presumed to be chemisorption accompanied by valence forces through electron sharing or exchange between RCS and As(V) as covalent forces [24]. This promotes the electrostatic attraction of As(V) ions towards the RCS, increasing biosorption. However, as a result of examining the equilibrium uptake, rate constant, and initial sorption rate of As(V), the effect of chitosan content in RCS was not significant. Considering the price of chitosan, the chitosan content for producing biosorbent economically was determined to be 4.0.

3.2.3. Effect of Biosorbent Size

The diameter size of the biosorbent is an important controlling parameter of the biosorption process. The effect of RCS diameter size on As(V) biosorption was studied using samples of four biosorbents with average diameters of 0.2–0.3, 0.5–0.6, 0.8–0.9, and 1.0–1.2 mm. The results are presented in Figure 1d. The equilibrium uptake values were similar (Table 2); however, the rate constant and initial sorption rate decreased when the biosorbent diameter increased from 0.2–0.3 to 1.0–1.2 mm. The higher biosorption with a smaller RCS diameter may be attributed to the fact that RCS with a smaller diameter has a greater surface area. Therefore, an RCS diameter size of 0.2–0.3 mm was selected for experimental purposes.

3.3. Adsorption Study

3.3.1. Kinetics

Figure 2 shows the kinetics of metalloid/metal adsorption on RCS as a function of batch contact time. The time to reach equilibrium was different for each metal. For cationic Cd(II), equilibrium was reached after 1 h. As(V) and Cr(VI) sorption was achieved after 3 h of contact time, respectively. The Mn(VII) sorption was finished after 6 h. Table 3 shows that the pseudo-second-order equation, which agrees that chemisorption is the rate-controlling mechanism, was better able to describe the adsorption of As(V), Cd(II), Cr(VI), and Mn(VII) onto RCS. Comparing the amount of adsorbed metal at equilibrium, the order is Mn(VII) > Cr(VI) > As(V) > Cd(II). Notably, the removal of Mn(VII) did not fit the kinetic models for adsorption (Table 3). This means that the Mn(VII) removal mechanism is different from other metals. To investigate the Mn(VII) removal characteristics of RCS, changes in total Mn concentration were investigated (Figure S3). Even after the complete removal of Mn(VII), some Mn remained in the aqueous phase. That is, the Mn remaining in the aqueous phase was Mn obtained by oxidation of Mn(VII). That is to say, some of the Mn(VII) was reduced to other oxidation states of Mn [25]. Cd(II) showed the fastest adsorption, although its adsorption capacity was smaller than that of other metals. In general, carboxyl groups present on biomass are known to be involved in the adsorption of Cd(II) [26].

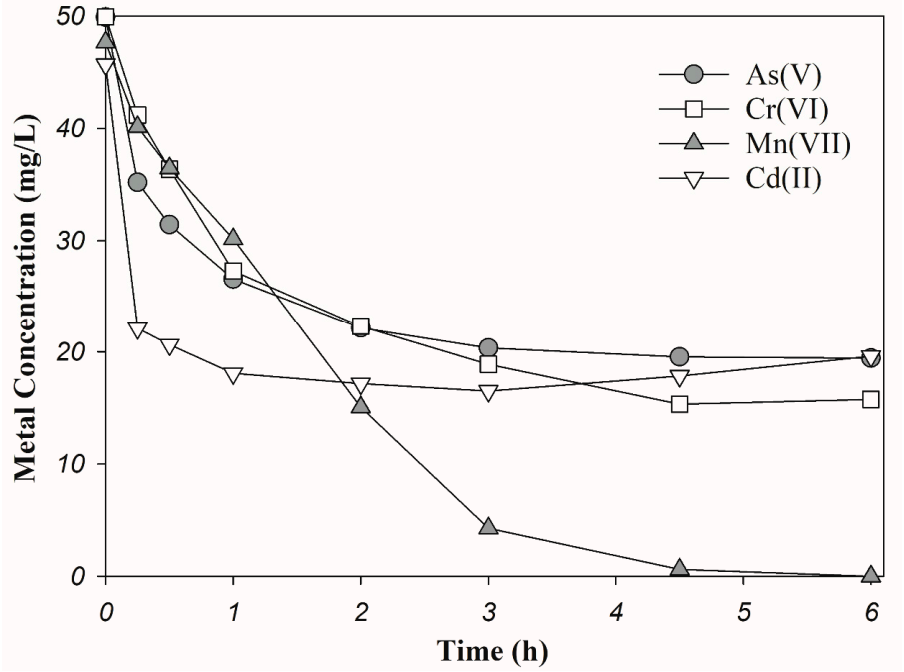

Figure 2. Kinetics of metalloid/metal adsorption (As(V), Cd(II), Cr(VI), and Mn(VII)) onto the sludge–chitosan (biomass dosage = 2 g/L, agitation rate = 200 rpm, contact time = 6 h, temperature = 25 °C, Vw = 200 mL, and pH non shift (pH 5.5)).

Table 3. Kinetic and isotherm constants for the biosorption of As(V), Cd(II), Cr(VI), and Mn(VII) by RCA.

		Pseudo-First-Order			Pseudo-Second-Order			
Kinetic	**Metals**	K_1 **(1/h)**	q_e **(mg/g)**	R^2 **(-)**	K_2 **(g/mg·h)**	q_e **(mg/g)**	R^2 **(-)**	h **(mg/g·h)**
	As(V)	0.85	8.64	0.9924	0.18	16.21	0.9996	47.68
	Cd(II)	0.51	2.91	0.8452	0.80	14.96	0.9999	178.06
	Cr(VI)	1.33	38.27	0.9840	0.06	19.94	0.9974	23.06
	Mn(VII)	1.02	34.94	0.9642	0.01	34.75	0.9645	14.66
		Langmuir			**Freundlich**			
Isotherm	**Metals**	Q_{max} **(mg/g)**	b **(L/mg)**	R^2 **(-)**	K_F **(mg/g)**	n	R^2 **(-)**	
	As(V)	42.25	0.0241	0.9711	6.3703	3.18	0.8643	
	Cd(II)	28.69	0.0398	0.8030	4.5064	2.94	0.9048	
	Cr(VI)	70.79	0.0201	0.9648	7.0609	2.57	0.8447	
	Mn(VII)	275.43	0.0163	0.8948	14.1749	1.98	0.9766	

3.3.2. Isotherms

Biosorption isotherms can represent the interaction between a biosorbate and biosorbent, and provide information about the distribution of the biosorbate between the liquid and solid phases at several equilibrium concentrations. Isotherm modeling is therefore important for biosorption data interpretation and prediction [7,27]. In this study, isotherm Freundlich and Langmuir models were used to evaluate biosorption equilibrium data. The Freundlich and Langmuir isotherm equations are as follows:

$$q_e = K_F C_e^{1/n} \quad (5)$$

and

$$q_e = \frac{q_{max} b C_e}{1 + b C_e} \quad (6)$$

where K_F and n are constants incorporating all parameters affecting the biosorption process in the Freundlich equation and b is the constant related to the affinity of the binding sites in the Langmuir equation. In the Freundlich equation, K_F $(L/mg)^{1/n}$ and n (dimensionless) are constants. On average, favorable adsorption tends to have an n between 1 and 10. In the Langmuir equation, q_{max} is the maximum adsorption capacity (mg/g) and b (L/g) is the isotherm constant.

The Langmuir and Freundlich isotherm models were used to interpret the experimental isotherm data of RCS. The model parameters and R^2 values are summarized in Table 3. The sorption experimental data and respective Langmuir and Freundlich isotherms are plotted in Figure 3a–d, respectively. A linear regression of the experimental results for As(V) and Cr(VI) proved a better fit in Langmuir isotherms. This result can be attributed to the fact that As(V) and Cr(VI) biosorption of RCS can be assumed by sorbate, and the equation describing the reaction rate allows for simultaneous adsorption and desorption [28]. When comparing the Langmuir parameter values obtained for As(V) and Cr(VI), q_{max} was approximately 42.25 mg As(V) or 70.79 mg Cr(VI) per g of RCS. The values for As(V) from the present study are comparable to or considerably greater than other reported sludge sorbents (Table 4). Various types of adsorbents (pyrolyzed form, biochar, alginate immobilized form, and magnetic sludge composite) were prepared from wastewater sludge, and their As(V) removal performance was 0.07–21.79 mg/g [29–33]. That is, RCS has a very high As(V) removal performance compared to existing adsorbents made from wastewater sludge. However, since RCS is structurally unstable below pH 5 (Figure S1), it has the weakness that it must be used at pH 5.5 or higher. Since As(V) exists as an anion, the adsorption efficiency decreases when the pH is high. Generally, the standard for wastewater discharge is pH 5.8 to 8.6. Therefore, the optimal operating condition for the As(V) removal process using RCS will be pH 5.5. The other metals, Cd(II) and Mn(VII), were well described by the Freundlich equation based on R^2. This difference can be explained by the existence of operating mechanisms other than basic ion exchange, such as specific adsorption–complexation reactions that occur during the adsorption process [34].

Table 4. Maximum uptakes of metals (As(V) and Cd(II)) by various biosorbents manufactured from sludge.

Metals	Sorbent Type	Uptake (mg/g)	Experimental Condition	Reference
As(V)	Pyrolyzed sludge (Industry)	0.07	pH 3.0–3.5, 48 h	[30]
	Biochar sewage sludge (Domestic)	13.42	pH 6.7–7, 24 h	[31]
	Acid mine drainage sludge (Industry)	21.50	pH 7, 24 h	[32]
	Acid mine drainage sludge alginate bead (Industry)	21.79	pH 5, 96 h	[33]
	Magnetic sludge composite (Domestic)	21.3	pH 2.6, 5 h	[34]
	Sludge–chitosan (Domestic)	42.25	pH 5.5, 6 h	This study
Cd(II)	Activated sludge (Domestic)	28.10	pH 5, 2 h	[35]
	Sewage sludge (Domestic)	28.41	pH 5, 24 h	[36]
	Sludge–chitosan (Domestic)	28.69	pH 5.5, 6 h	This study

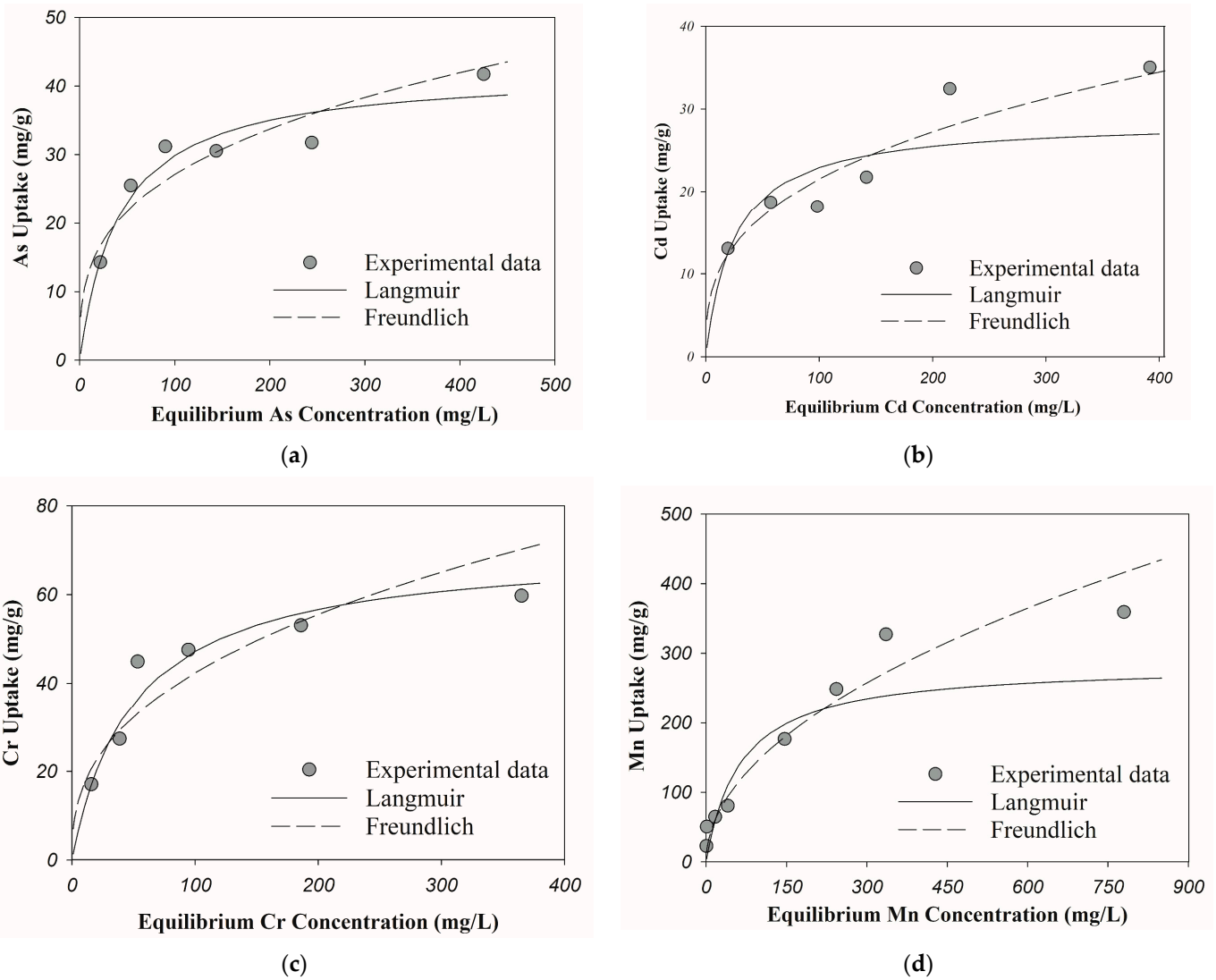

Figure 3. Adsorption isotherms of (**a**) As(V), (**b**) Cd(II), (**c**) Cr(VI), and (**d**) Mn(VII) by the rod-type biosorbent. The continuous lines were predicted by the Langmuir model; the dotted lines were produced by the Freundlich model (biomass dosage = 2 g/L, agitation rate = 200 rpm, temperature = 25 °C, Vw = 200 mL, and pH non shift (pH 5.5)).

4. Conclusions

The purpose of this study was to develop a high-performance biosorbent from non-living activated sludge generated in the wastewater treatment process. The problem of elution of organic matter from the sludge was solved through the immobilization method using chitosan. Based on the As(V) removal performance, the optimal conditions for the preparation of chitosan-based biosorbents were derived: 6.0% dry sludge, 4.0% chitosan, and a rod shape with a diameter of 0.2–0.3 mm. Investigation of the removal rates of various cationic and anionic heavy metals showed that the biosorbent adsorbed anionic metals more effectively than cationic metals. The maximum removal capacities of RCS were determined to be 42.25 mg/g for As(V), 28.69 mg/g for Cd(II), 70.79 mg/g for Cr(VI), and 284.11 mg/g for Mn(VII). Since this is a basic study, it is not appropriate to mention the practical applicability of RCS at this point. That is, a solution to the problem of non-acid resistance is required for the commercialization of RCS. Studies related to adsorbent regeneration and disposal should be also performed. In addition to these follow-up studies, the results of this study will be useful for commercially producing adsorbents for heavy metal removal using wastewater sludge in the future.

Supplementary Materials: The following supporting information can be downloaded at: https://www.mdpi.com/article/10.3390/app13042055/s1, Figure S1: Stability of chitosan-immobilized biosorbents as a function of solution pH; Figure S2: Fourier transform infrared absorption spectra of raw sludge and sludge-immobilized chitosan; Figure S3: Mn concentration profiles during Mn(VII) biosorption by RCS.

Author Contributions: J.H.S.: methodology, formal analysis; N.K.: conceptualization, writing—original draft preparation; M.P.: investigation, methodology; D.P.: supervision, writing—review and editing. All authors have read and agreed to the published version of the manuscript.

Funding: This research was supported by the Basic Science Research Program through the National Research Foundation of Korea (NRF) funded by the Ministry of Education (No. 2021R1I1A1A01050092).

Institutional Review Board Statement: Not applicable.

Informed Consent Statement: Not applicable.

Data Availability Statement: The datasets used and analyzed during the current study are available from the corresponding author on reasonable request.

Conflicts of Interest: The authors declare no conflict of interest.

References

1. Fu, F.; Wang, Q. Removal of heavy metal ions from wastewaters: A review. *J. Environ. Manag.* **2011**, *92*, 407–418. [CrossRef] [PubMed]
2. Yaqub, M.; Lee, S.H. Heavy metals removal from aqueous solution through micellar enhanced ultrafiltration: A review. *Environ. Eng. Res.* **2019**, *24*, 363–375. [CrossRef]
3. Park, D.; Yun, Y.S.; Park, J.M. The past, present, and future trends of biosorption. *Biotechnol. Bioprocess Eng.* **2010**, *15*, 86–102. [CrossRef]
4. Al-Qodah, Z. Biosorption of heavy metal ions from aqueous solutions by activated sludge. *Desalination* **2006**, *196*, 164–176. [CrossRef]
5. Maderova, Z.; Baldikova, E.; Pospiskova, K.; Safarik, I.; Safarikova, M. Removal of dyes by adsorption on magnetically modified activated sludge. *Int. J. Environ. Sci. Technol.* **2016**, *13*, 1653–1664. [CrossRef]
6. Ozdemir, S.; Turp, S.M.; Oz, N. Simultaneous dry-sorption of heavy metals by porous adsorbents during sludge composting. *Environ. Eng. Res.* **2020**, *25*, 258–265. [CrossRef]
7. Seo, J.H.; Kim, N.; Park, M.; Lee, S.; Yeon, S.; Park, D. Evaluation of metal removal performance of rod-type biosorbent prepared from sewage-sludge. *Environ. Eng. Res.* **2020**, *25*, 700–706. [CrossRef]
8. Dai, Y.; Zhang, N.; Xing, C.; Cui, Q.; Sun, Q. The adsorption, regeneration and engineering applications of biochar for removal organic pollutants: A review. *Chemosphere* **2019**, *223*, 12–27. [CrossRef]
9. Lin, X.; Wang, L.; Jiang, S.; Cui, L.; Wu, G. Iron-doped chitosan microsphere for As(III) adsorption in aqueous solution: Kinetic, isotherm and thermodynamics studies. *Korean J. Chem. Eng.* **2019**, *36*, 1102–1114. [CrossRef]
10. Vijayaraghavan, K.; Yun, Y.-S. Bacterial biosorbents and biosorption. *Biotechnol. Adv.* **2018**, *26*, 266–291. [CrossRef]
11. Gerente, C.; Lee, V.K.C.; Le Cloirec, P.; McKay, G. Application of chitosan for the removal of metals from wastewaters by adsorption—Mechanisms and models review. *Crit. Rev. Environ. Sci. Technol.* **2007**, *37*, 41–127. [CrossRef]
12. Kim, N.; Park, M.; Park, D. A new efficient forest biowaste as biosorbent for removal of cationic heavy metals. *Bioresour. Technol.* **2015**, *175*, 629–632. [CrossRef]
13. Deng, S.; Ting, Y.P. Polyethylenimine-modified fungal biomass as a high-capacity biosorbent for Cr(VI) anions: Sorption capacity and uptake mechanisms. *Environ. Sci. Technol.* **2005**, *39*, 8490–8496. [CrossRef]
14. Keyvani, F.; Rahpeima, S.; Javanbakht, V. Synthesis of EDTA-modified magnetic activated carbon nanocomposite for removal of permanganate from aqueous solutions. *Solid State Sci.* **2018**, *83*, 31–42. [CrossRef]
15. Amrullah, A.; Paksung, N.; Matsumura, Y. Cell structure destruction and its kinetics during hydrothermal treatment of sewage sludge. *Korean J. Chem. Eng.* **2019**, *36*, 433–438. [CrossRef]
16. Altun, T.; Ecevit, H. Cr(VI) removal using Fe_2O_3-chitosan-cherry kernel shell pyrolytic charcoal composite beads. *Environ. Eng. Res.* **2000**, *25*, 426–438. [CrossRef]
17. Chen, Q.; Zheng, J.; Wen, L.; Yang, C.; Zhang, L. A multi-functional-group modified cellulose for enhanced heavy metal cadmium adsorption: Performance and quantum chemical mechanism. *Chemosphere* **2019**, *224*, 509–518. [CrossRef] [PubMed]
18. Ramrakhiani, L.; Majumder, R.; Khowala, S. Removal of hexavalent chromium by heat inactivated fungal biomass of *Termitomyces clypeatus*: Surface characterization and mechanism of biosorption. *Chem. Eng. J.* **2011**, *171*, 1060–1068. [CrossRef]
19. Kim, N.; Park, M.; Yun, Y.-S.; Park, D. Removal of anionic arsenate by a bacterial biosorbent prepared from fermentation biowaste. *Chemosphere* **2019**, *226*, 67–74. [CrossRef]

20. Lipatova, I.M.; Makarova, L.I.; Yusova, A.A. Adsorption removal of anionic dyes from aqueous solutions by chitosan nanoparticles deposited on the fibrous carrier. *Chemosphere* **2018**, *212*, 1155–1162. [CrossRef] [PubMed]
21. Ho, Y.S. Review of second-order models for adsorption systems. *J. Hazard. Mater.* **2006**, *136*, 681–689. [CrossRef] [PubMed]
22. Ho, Y.S.; McKay, G. Pseudo-second order model for sorption processes. *Process Biochem.* **1999**, *34*, 451–465. [CrossRef]
23. Tran, H.N.; You, S.-J.; Hosseini-Bandegharaei, A.; Chao, H.-P. Mistakes and inconsistencies regarding adsorption of contaminants from aqueous solutions: A critical review. *Water Res.* **2017**, *120*, 88–116. [CrossRef]
24. Graillot, A.; Bouyer, D.; Monge, S.; Robin, J.J.; Loison, P.; Faur, C. Sorption properties of a new thermosensitive copolymeric sorbent bearing phosphonic acid moieties in multi-component solution of cationic species. *J. Hazard. Mater.* **2013**, *260*, 425–433. [CrossRef] [PubMed]
25. Dash, S.; Patel, S.; Mishra, B.K. Oxidation by permanganate: Synthetic and mechanistic aspects. *Tetrahedron* **2009**, *65*, 707–739. [CrossRef]
26. Su, J.; Gao, C.; Huang, T.; Gao, Y.; Bai, X.; He, L. Characterization and mechanism of the Cd(II) removal by anaerobic denitrification bacterium *Pseudomonas* sp. H117. *Chemosphere* **2019**, *222*, 970–979. [CrossRef]
27. Ren, Z.; Chen, F.; Wang, B.; Song, Z.; Zhou, Z.; Ren, D. Magnetic biochar from alkali-activated rice straw for removal of rhodamine B from aqueous solution. *Environ. Eng. Res.* **2020**, *25*, 536–544. [CrossRef]
28. Saeed, A.; Iqbal, M.; Akhtar, M.W. Removal and recovery of lead(II) from single and multimetal (Cd, Cu, Ni, Zn) solutions by crop milling waste (black gram husk). *J. Hazard. Mater.* **2005**, *117*, 65–73. [CrossRef] [PubMed]
29. Tavares, D.S.; Lopes, C.B.; Coelho, J.P.; Sánchez, M.E.; Garcia, A.I.; Duarte, A.C.; Otero, M.; Pereira, E. Removal of arsenic from aqueous solutions by sorption onto sewage sludge-based sorbent. *Water Air Soil Pollut.* **2012**, *223*, 2311–2321. [CrossRef]
30. Agrafioti, E.; Kalderis, D.; Diamadopoulos, E. Arsenic and chromium removal from water using biochars derived from rice husk, organic solid wastes and sewage sludge. *J. Environ. Manag.* **2014**, *113*, 309–314. [CrossRef] [PubMed]
31. Yang, J.S.; Kim, Y.S.; Park, S.M.; Baek, K. Removal of As(III) and As(V) using iron-rich sludge produced from coal mine drainage treatment plant. *Environ. Sci. Pollut. Res.* **2014**, *21*, 10878–10889. [CrossRef] [PubMed]
32. Lee, H.; Kim, D.; Kim, J.; Ji, M.K.; Han, Y.S.; Park, Y.T.; Yun, H.S.; Choi, J. As(III) and As(V) removal from the aqueous phase via adsorption onto acid mine drainage sludge (AMDS) alginate beads and goethite alginate beads. *J. Hazard. Mater.* **2015**, *292*, 146–154. [CrossRef] [PubMed]
33. Wang, L.; Wang, J.M.; Zhang, R.; Liu, X.G.; Song, G.X.; Chen, X.F.; Wang, Y.; Kong, J.L. Highly efficient As(V)/Sb(V) removal by magnetic sludge composite: Synthesis, characterization, equilibrium, and mechanism studies. *RSC Adv.* **2016**, *6*, 42876–42884. [CrossRef]
34. Liu, H.; Yang, F.; Zheng, Y.; Kang, J.; Qu, J.; Chen, J.P. Improvement of metal adsorption onto chitosan/*Sargassum* sp. composite sorbent by an innovative ion-imprint technology. *Water Res.* **2011**, *45*, 145–154. [CrossRef] [PubMed]
35. Hammaini, A.; González, F.; Ballester, A.; Blázquez, M.L.; Muñoz, J.A. Biosorption of heavy metals by activated sludge and their desorption characteristics. *J. Environ. Manag.* **2007**, *84*, 419–426. [CrossRef] [PubMed]
36. Hu, J.-L.; He, X.-W.; Wang, C.-R.; Li, J.-W.; Zhang, C.-H. Cadmium adsorption characteristic of alkali modified sewage sludge. *Bioresour. Technol.* **2012**, *121*, 25–30. [CrossRef] [PubMed]

Disclaimer/Publisher's Note: The statements, opinions and data contained in all publications are solely those of the individual author(s) and contributor(s) and not of MDPI and/or the editor(s). MDPI and/or the editor(s) disclaim responsibility for any injury to people or property resulting from any ideas, methods, instructions or products referred to in the content.